ACS OMEGA

Open Access

http://pubs.acs.org/journal/acsodf

Article

Research on the Influence of Heterogeneity and Viscosity on the Fluid Intrusion Mechanism of the Water Flooding Process Based on the Microscopic Visualization Experiment

Jitao Wang, Junjian Li,* Yunsong Li, Runzi Xu, Guanghui Xu, and Jinlong Yang

Cite This: *ACS Omega* 2024, 9, 2866−2873

Read Online

ACCESS | Metrics & More | Article Recommendations

ABSTRACT: The flow law of immiscible fluids in porous media plays an important role in the development of oil and gas fields. In the process of water flooding reservoir development, when the water phase displaces the oil phase, a fluid with higher viscosity, as a fluid with lower viscosity, the oil−water interface will always be unstable, resulting in different fingering effects. After water flooding, the distribution law of oil and water in the reservoir is mainly affected by the fluid intrusion mechanism. Due to the difference of capillary force, viscous force, and other microscopic forces, the fluid intrusion mechanism is mainly divided into two types: viscous fingering and capillary fingering. At the same time, due to the influence of reservoir heterogeneity, the fingering effect in the process of water displacement in porous media will be influenced to a certain extent. Based on the two-dimensional microscopic visualization experiment, this paper extracted the variance of the static parameter G in the capillary number calculation method of the two-dimensional microscopic model to represent the heterogeneity and conducted displacement experiments with different viscosities and flow rates to study the influence of the flow rate, viscosity, and heterogeneity on the results of water flooding. The experiments found that as for the influence of flow velocity, with the increase of flow velocity, that is, with the increase of capillary number, the recovery degree decreases first and then increases. As for the influence of viscosity, from a numerical point of view, the displacement efficiency and conformance coefficient of the low-viscosity group are higher than those of the high-viscosity group. From the trend, with the increase of the capillary number, the displacement efficiency of both the low-viscosity and high-viscosity groups increases, while the conformance coefficient decreases first and then increases, indicating that capillary fingering and viscous fingering can occur in different viscosity reservoirs. As for the influence of heterogeneity, the conformance coefficient of the water flooding decreases with the increase of heterogeneity, and the viscous pointing trend caused by heterogeneity is stronger, resulting in an uneven water injection sweep and higher oil displacement efficiency within the swept area. It can be seen from the fluid intrusion mechanism diagram that with the increase of heterogeneity, the viscous fingering trend becomes more obvious; with the increase of viscosity, the fluid intrusion mechanism boundary moves down and the viscous fingering trend becomes more obvious.

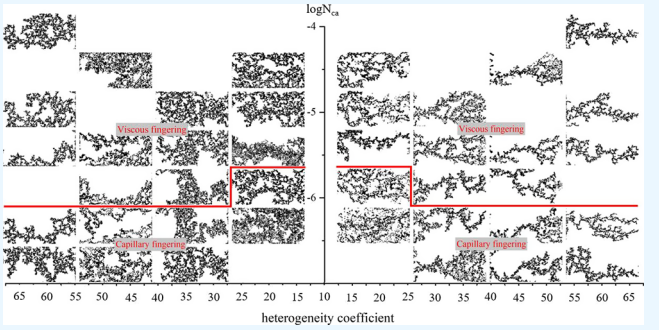

1. INTRODUCTION

The flow of immiscible fluid in porous media plays an important role in the development of oil and gas reservoirs. In the process of reservoir water flooding production, when the water phase displaces the oil phase with high viscosity as a fluid with low viscosity, the oil−water interface will always be unstable, resulting in different mechanisms of fluid invasion, the fingering effect. In the past 50 years, immiscible fluid flow in porous media has been the focus of research. As early as 1983, the scholar Lenorman studied the process of wetting phase displacement and nonwetting phase displacement through microscopic glass models and found that the flow process was affected by viscosity, displacement velocity and interfacial tension.[1] The scholar He also found in the gas−water flow experiment that, at a local scale, the curved fluid−fluid interface would be subject to the complex interaction of capillary force and viscous force.[2] Therefore, determining how to classify and characterize the mechanisms of fluid invasion is a key problem. Lenormand et al. put forward the basic phase diagram of the mechanisms of fluid invasion in porous media through numerical simulation and microscopic experiments

Received: October 22, 2023
Revised: December 13, 2023
Accepted: December 15, 2023
Published: January 4, 2024

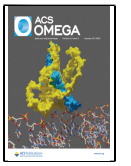

and divided the mechanisms of fluid invasion into complete displacement, viscous fingering, and capillary fingering.[3] There were transition regions between each mode, and a new method was established using two key dimensionless numbers. Namely, the capillary number ($N_{ca} = v\mu_i/\sigma$) and viscosity ratio ($M = \mu_i/\mu_d$) to show how competition between capillary and viscous forces affects the flow pattern, where μ_i and μ_d are the viscosity of the displaced and displaced phases, respectively, v is the characteristic velocity of the invading fluid, and σ is the interfacial tension of the fluid. Under unfavorable conditions ($M < 1$) (displacing phase is a nonwetting phase), the mechanism of fluid invasion transitions from capillary finger-in to viscous finger-in with increasing capillary number Ca, while under favorable conditions ($M > 1$), the mechanism of fluid invasion transitions from capillary finger-in to complete displacement with increasing capillary number Ca. Zhang et al. confirmed the simulation results of Lenormand et al. through micromodel displacement experiments with different capillary numbers and viscosity ratios.[4] Holtzman and Segre took the influence of wettability into account in the displacement process and found that as the wettability of the displacement phase increased, the displacement front became more stable, and this effect decreased with the increase of flow velocity.[5] Zhao et al. studied the influence of wettability on the fingering effect in heterogeneous media through microscopic visualization experiments. Fluid−fluid displacement under the condition of high capillary number is mainly caused by the formation of a wetting film on a solid surface, which leads to incomplete displacement at the pore scale.[6] Hu et al. also found this phenomenon in the process of gas−liquid displacement.[7] Or used dimensionless force ratio represented by viscous force and capillary number to describe the morphology of displacement fluid front in the process of describing the change of displacement fluid front and also considered the influence of gravity.[8] Holtzman and Juanes took the crack effect into account when describing the flow of immiscible fluids in porous media and established a dimensionless parameter to distinguish the influence of viscous fingering from the crack effect.[9] All of these studies show how the competition between capillary and viscous forces affects the mechanism of fluid invasion, taking into account the effects of wettability, gravity, and cracks. However, if the influence of pore-scale heterogeneity is taken into account, then the mechanism of the fluid invasion evolution process will be more complicated. From the perspective of the sweep, heterogeneity on the pore scale will affect the fluid flow path and, thus, affect the finger shape. From the perspective of oil displacement efficiency, the capillary force distribution caused by heterogeneity and the water flooding path are different, resulting in the displacement of large and small holes with different pore radii. How to characterize the role of heterogeneity in the evolution of the mechanism of fluid invasion is very critical.

Heterogeneity exists widely in porous media in different forms, and the definition of heterogeneity varies from macro to micro and from field scale to pore scale. At the field scale, Yang et al. used the Weibull distribution function and convective dispersion model to evaluate the influence of permeability and porosity heterogeneity on liquid intrusion in tight gas reservoirs.[10] At the pore scale, Dou and Zhou used the improved lattice Boltzmann method (LBM) to study the effects of capillary number Ca and viscosity ratio M on the relative permeability (RP)−wetting saturation (S_w) relationship of the steady-state immiscible two-phase flow in heterogeneous porous media.[11] So how to connect the heterogeneity with the change of the mechanism of fluid invasion is a problem worth thinking about. Chen and Wilkinson studied the relationship between viscous pointing and heterogeneity in porous media and found that the increase in heterogeneity would lead to the instability of the displacement front.[12] On this basis, King selected the change of pore radius λ as the parameter to characterize heterogeneity and the fractal dimension as the index to quantify the relationship between heterogeneity and fingering morphology.[13] Hu et al. also selected the change of pore radius λ as a parameter to characterize heterogeneity and proposed a theoretical model to describe the upper and lower boundaries of capillary fingering and viscous fingering as well as their intersecting regions under specific heterogeneity conditions. It was found that the intersecting regions expanded with the increase of heterogeneity.[14] Holtzman et al.took the difference in the distance distribution between the mesh particles in the microscopic model as the heterogeneity characterization parameter and quantitatively evaluated the effect of pore diameter heterogeneity and its interaction with flow rate and wettability on viscous fluid immiscible displacement.[15] From previous studies, it can be found that many efforts have been made to establish the quantitative relationship between heterogeneity and mechanisms of fluid invasion, such as viscous fingering and capillary fingering. This paper attempts to establish the relationship between the capillary number and heterogeneity coefficient from another perspective based on the calculation method of the capillary number based on the two-dimensional microscopic model, taking the variance of static parameters of the two-dimensional microscopic model as the heterogeneity index, so as to determine the influence of different heterogeneities on the evolution rule of the mechanism of fluid invasion under different viscosity conditions. The mechanism of the fluid invasion boundary was constructed with heterogeneity and capillary number as indexes. Through the research of the fluid intrusion mechanism of the microscopic visualization experiment, the form of water flooding pointing can be determined under different viscosity and different capillary numbers, so as to select the most appropriate water flooding speed, so that the injected water can be more effective in sweeping and displacement.

2. MATERIALS AND METHODS

2.1. Experimental Method. The displacement water used in the experiment was deionized water, which was dyed blue with methylene blue. The crude oil used in the low-viscosity group was 3# industrial white oil with a viscosity of 2.909 mP·s measured at 25 °C, and the crude oil used in the high-viscosity group was 100# industrial white oil with a viscosity of 109.246 mP·s measured at 25 °C. The experimental oil was dyed red with Sudan IV, which was convenient for observation and image processing. Considering that the number of pore throats of the two-dimensional microscopic model obtained by mask etching directly using cast thin slice images is small, the displacement results are more accidental, which cannot reflect the real flow situation. Therefore, in this paper, the Quartet structure generation set technique is used to generate four different heterogeneous microscopic two-dimensional model masks with the same pore structure as the cast sheet. Finally, an experimental microscopic glass model is obtained through

https://doi.org/10.1021/acsomega.3c08205
ACS Omega 2024, 9, 2866−2873

wet etching. The glass model size is 10 cm x 10 cm, and the model pattern length is 30 mm. The width is 15 mm and the etching depth is 30 μm.

The experimental operation equipment consisted of a constant current microinjection pump and a Leica M165FC stereo microscope equipped with a Leica DF450C camera. Before the start of the experiment, propanol and deionized water were used to wash the inside of the microscopic model. After the plates were washed, a displacement experiment was carried out. The experiment included the following steps:

1. Saturated water: The microinjection pump is used to slowly inject simulated formation water into the micromodel so that the pores and throats of the model are saturated with water.
2. Saturated oil: The microinjection pump is used to slowly inject experimental oil with a certain viscosity into the saturated water model, so that the simulated oil will drive out the flowing water in the pores of the model until there is no more water out of the outlet, and the injection will stop. At this time, the model is in a state of saturated oil and bound water.
3. Water flooding: A microinjection pump is used to inject about 3PV of experimental displacement water at different speeds and take photos to record the process.
4. The ultimate recovery factor should be calculated and the distribution of the remaining oil should be analyzed.

Based on the microscopic displacement experiment, a total of 40 groups of microfluidic experiments were designed, taking into account the factors affecting different viscosities, heterogeneities, and displacement velocity. The N_{ca} calculation method for the two-dimensional displacement model was used to calculate the capillary number and heterogeneity coefficient of each group, and the flow mode under the influence of heterogeneity was classified and characterized according to the experimental results.

2.2. Heterogeneity Coefficient Characterization Method. Tang et al. found that the calculation of the capillary number of two-dimensional microscopic models is different from conventional calculation methods, and the representation methods can be divided into expressions based on permeability and expressions based on the experimental flow rate.[16] The calculation equation can be divided into two parts: one is the model-related static parameters and the other is the experiment-related dynamic parameters:

Expression based on permeability:

$$N_{ca} = \left(\frac{k|\nabla p|}{\sigma\cos\theta}\right)\left[\left(\frac{12}{2}\right)\left(\frac{W_t}{d_z}\right)^2\left(\frac{L_p}{W_t}\right)\frac{1}{\left(1-\frac{W_t}{W_b}\right)(\varphi\xi)}\right] \quad (1)$$

Expression based on the experimental flow rate:

$$N_{ca} = \left(\frac{u\mu}{\sigma\cos\theta}\right)\frac{1}{k_{rw}}\left[\left(\frac{12}{2}\right)\left(\frac{W_t}{d_z}\right)^2\left(\frac{L_p}{W_t}\right)\frac{1}{\left(1-\frac{W_t}{W_b}\right)(\varphi\xi)}\right] \quad (2)$$

In formulas 1 and 2, $\left(\frac{12}{2}\right)\left(\frac{W_t}{d_z}\right)^2\left(\frac{L_p}{W_t}\right)\frac{1}{\left(1-\frac{W_t}{W_b}\right)(\varphi\xi)}$ are static parameters, expressed by G, and the rest are dynamic parameters. The statistical methods of parameters are shown in Table 1.

Table 1. Summary of Parameters Needed for the Calculation of N_{ca}

experiment number	model parameters	remarks
geometrical factors	characteristic pore-throat width, W_t	statistical average of pore-throat distribution
	characteristic pore-body diameter, W_b	statistical average of pore-body distribution
	pore length, L_p	roughly identical to W_b in the networks considered here
fluid and media properties	wettability, indicated by contact angle, θ	measured in lab
	interfacial tension between phases, σ	measured in lab
flow data	pressure gradient, ∇p	measured via flow experiments

For the two-dimensional microscopic model, pore size is the main factor affecting the remaining oil reservoir capacity, while the throat width mainly affects the fluid migration capacity. Therefore, the variance of the static parameter G of the model can be selected to characterize the heterogeneity of the two-dimensional microscopic model, which can be expressed as (f), as shown below. In the equation, the pore width is represented by the average value and is substituted into the throat width for calculation. The pore size and throat size can be obtained by image processing.

$$f = \sqrt{\frac{1}{N}\sum_{i=1}^{N}(G_i - \bar{G})^2} \quad (3)$$

2.3. Experimental Results' Image Processing. At the beginning and end of the experiment, the two-dimensional microscopic model was photographed with a resolution of 2560 × 1920. It should be noted that the relative position of the lens and the two-dimensional microscopic model should not be moved during the experiment; otherwise, the saturated oil image and the water flooding result image could not be aligned, resulting in the error of remaining oil identification. In order to ensure more accurate image processing results, the experimental photos were intercepted, and only the image part of the two-dimensional microscopic model was captured, and the size of the captured image was 1190 × 630. Then, based on the remaining oil classification, identification, and statistical analysis software, the photos of the saturated oil stage are input, and the model throat and rock skeleton are automatically identified through the software binarization function, and the photos of water flooding results are input, and the oil, water, and rock skeleton are automatically identified through the software ternary function. Finally, the types and contents of the remaining oil in different pore radii can be obtained through the remaining oil classification, identification, and statistical function. Through ImageJ software, the water flooding result image is transformed into the gray level map, and the water flow path is extracted based on gray level distribution to form a binary map of the water flooding result.

3. RESULTS AND DISCUSSION

3.1. Effect of Flow Velocity on Water Flooding Results. Taking the homogeneous group as an example, the oil viscosity in this experiment is 2.909 mP·s, a total of five

https://doi.org/10.1021/acsomega.3c08205
ACS Omega 2024, 9, 2866−2873

displacement velocity gradients were designed, ranging from the minimum 0.05 μL/min to the maximum 1.00 μL/min, and the capillary number ranged from 1.62×10^{-6} to 3.24×10^{-5}. Observing the process of water flooding, it can be seen that at a low speed, as shown in Figure 1, water is subjected to capillary

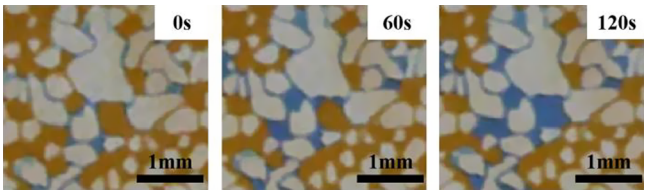

Figure 1. Launching process under low-viscosity homogeneous group conditions.

imbibition and first enters the small hole to form a water film. With the subsequent supplementation of water, the water film expands to fill the pores and extrude oil. At this time, the effect of the capillary force is obvious. However, the situation is very different in high-speed displacement; when water mainly flows along the large pores, the small pores no longer fill, and the viscous finger is formed along the direction of the large pores. At this time, the viscous force is obvious.

It can also be seen from the comparison of water flooding results as shown in Figure 2 that after low-speed displacement,

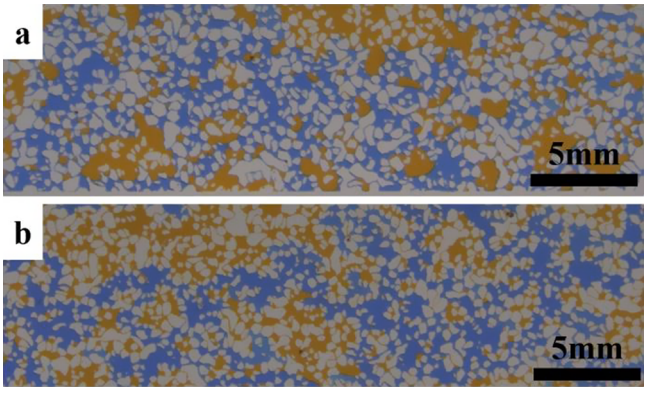

Figure 2. Results of low-speed (a, 0.05 μL/min, $N_{ca} = 1.62 \times 10^{-6}$) and high-speed (b, 1.00 μL/min, $N_{ca} = 3.24 \times 10^{-5}$) water flooding in the homogeneity−low-viscosity group.

the remaining oil in the small pores in the swept area has a better displacement effect, while in the large pores, because of the low viscosity, there is even isolated remaining oil, which cannot move out of the large pores. In high-speed water flooding, the displacement of water flows along the macropores to form a viscous finger. In the macropores that have been swept, the oil displacement efficiency is higher; the remaining oil is driven clean, and the small pores around the macropores are poorly swept. Through the statistics of remaining oil utilization in different pore sizes, it can be found that, as shown in Figure 3, the degree of small pore utilization is higher at low speed, that is, $N_{ca} = 4.97 \times 10^{-7}$, and the degree of large pore utilization is higher at high speed, that is, $N_{ca} = 9.93 \times 10^{-6}$. The limit of 150 μm is used for comparison. The degree of water driving at low speed is 13.71% higher than that at high speed, and the degree of water driving at high speed is 8.2% higher than that at low speed for pores larger than 150 μm.

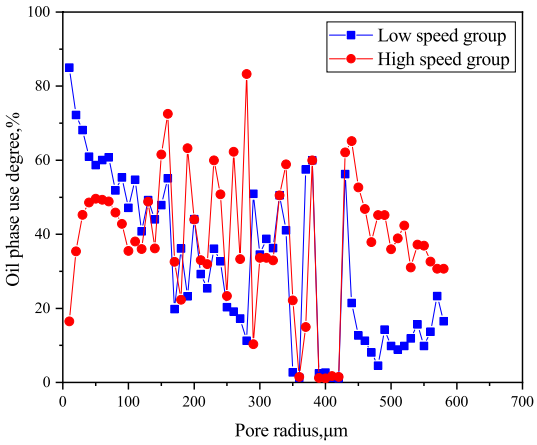

Figure 3. Statistics of utilization degree of different pore radii at high and low speeds in the homogeneity−low-viscosity group.

Based on the image processing and remaining oil statistics of displacement results at different water displacement speeds, the relationship between the recovery degree and capillary number of the homogeneous and low-viscosity groups at different displacement speeds was obtained, as shown in Figure 4. High

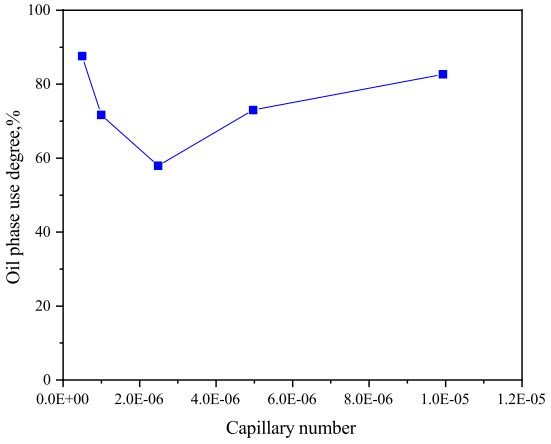

Figure 4. Curves of different capillary numbers in the homogeneity−low-viscosity group−recovery degree.

recovery degrees were achieved at both low speed and high speed, 87.61 and 82.66%, respectively. At the medium speed ($N_{ca} = 2.48 \times 10^{-6}$), the recovery degree was the lowest, only 57.94%. At low speed, with the increase of the water flooding speed, the degree of recovery decreases, which is capillary fingering; at medium and high speeds, with the increase of the water flooding speed, the degree of recovery increases, which is viscous fingering.

3.2. Effect of Viscosity on Water Flooding Results.

Taking the homogeneity and low-speed group as an example, as shown in Figure 5, comparing the displacement results of the low-viscosity group (2 mPa·s) and the high-viscosity group (150 mPa·s), it can be found that the oil displacement efficiency of the low-viscosity group is higher, and the oil phase is replaced by water phase in the affected pores; the oil displacement efficiency of the high-viscosity group is lower, and the water phase enters the pores and only brings out a part of the oil phase, and more oil phases are deposited in the pores in blocky or film form. The oil displacement efficiency of the swept area was calculated by image processing and was only

https://doi.org/10.1021/acsomega.3c08205
ACS Omega 2024, 9, 2866−2873

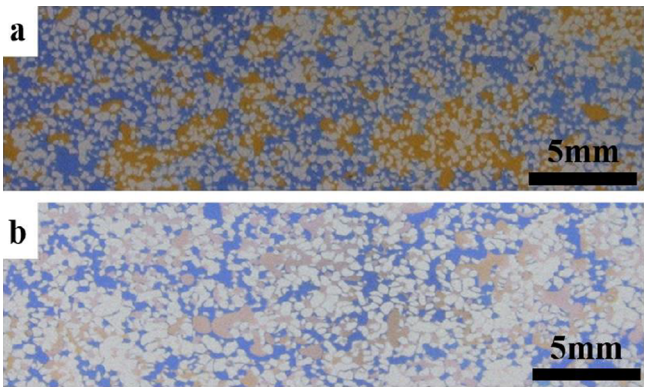

Figure 5. Results of low-viscosity (a, 2 mPa·s) and high-viscosity (b, 150 mPa·s) water flooding in the homogeneity−low-speed group.

71.36% in the high-viscosity group and 96.03% in the low-viscosity group. According to the statistics on the utilization of the remaining oil in different pore sizes, it can be found, as shown in Figure 6, that when the viscosity is different, the

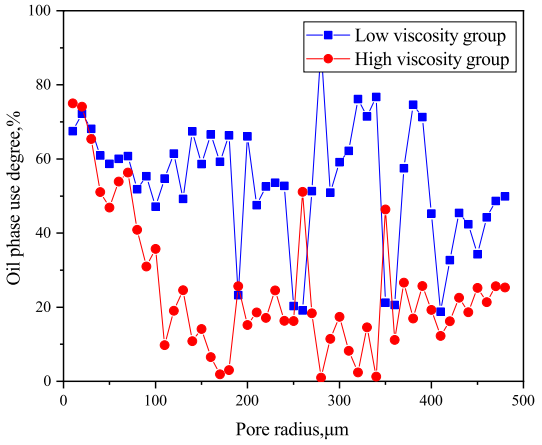

Figure 6. Statistics of utilization degree of different pore radii of high viscosity and low viscosity in the homogeneity−low-speed group.

utilization of small pores below 100um radius in the high-viscosity and low-viscosity groups is similar, while the utilization of large pores above 100um is significantly different, and the utilization of large pores in the high-viscosity group is poor.

Based on the image processing of displacement results under different viscosities and the statistics of the remaining oil, the relationship curves of oil displacement efficiency, sweep efficiency, and a capillary number of homogeneous and low-speed groups under different viscosities were obtained, as shown in Figure 7 With the increase of the capillary number, the oil displacement efficiency of both low-viscosity and high-viscosity groups increased, and the oil displacement efficiency of the high-viscosity group increased significantly when the same capillary number was increased, reaching 11.29%. In terms of the sweep, as shown in Figure 8, the overall sweep of the high-viscosity group is smaller than that of the low-viscosity group due to the relatively large water−oil mobility. With the increase of the capillary number, the sweep efficiency of both high-viscosity and low-viscosity groups decreases first and then increases, indicating that capillary fingering and viscous fingering can occur in different viscosity reservoirs.

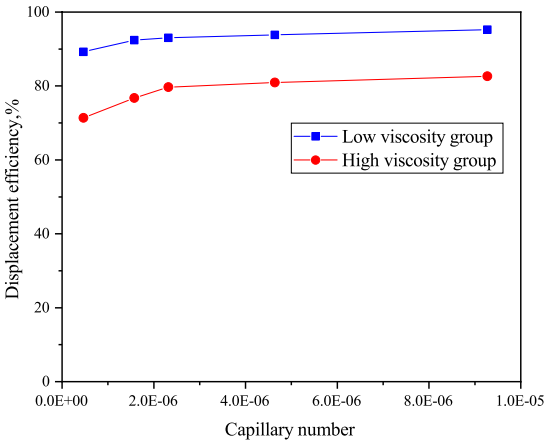

Figure 7. Capillary number and displacement efficiency curves of the homogeneous group with different viscosities.

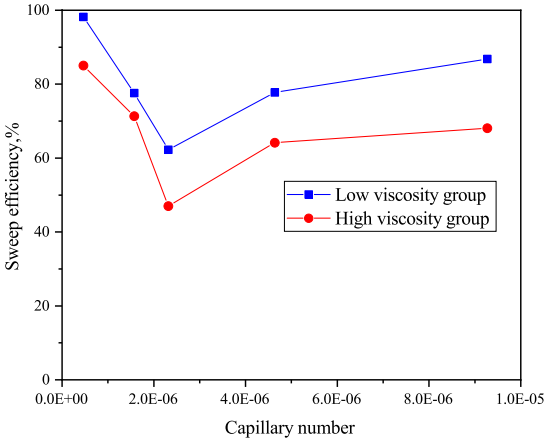

Figure 8. Capillary number and sweep efficiency curves of the homogeneous group with different viscosities.

3.3. Effect of Heterogeneity on Water Flooding Results. In this paper, heterogeneity is characterized by the variance of static parameter G of the model. With the increase of heterogeneity, the distribution of the pore throat radius becomes more uneven. Through the calculation of the variance of *G* values of the four models, the four models were defined as the homogeneous group, the weak heterogeneous group, the nonhomogeneous group, and the strong heterogeneous group from large to small according to the heterogeneity coefficient, whose heterogeneity coefficients were 15.27, 24.79, 32.32, and 62.62, respectively.

Taking the low-viscosity low-speed group as an example, as shown in Figure 9, the sweep coefficient of water flooding for the homogeneous group is 91.23%, while that for the strongly heterogeneous group is only 65.31%. With the increase of heterogeneity, the sweep coefficient of the water flooding decreases, and heterogeneity leads to the worse sweep of water flooding. From the perspective of oil displacement efficiency, viscous pointing caused by heterogeneity makes the injection water spread uneven, and the model with stronger heterogeneity is washed by more water in the swept area, resulting in higher oil displacement efficiency in the swept area. It can also be seen in Figure 10 that the oil displacement efficiency of the homogeneous group is only 91.04%, while the oil displacement efficiency of the nonhomogeneous group is 98.13%.

https://doi.org/10.1021/acsomega.3c08205
ACS Omega 2024, 9, 2866−2873

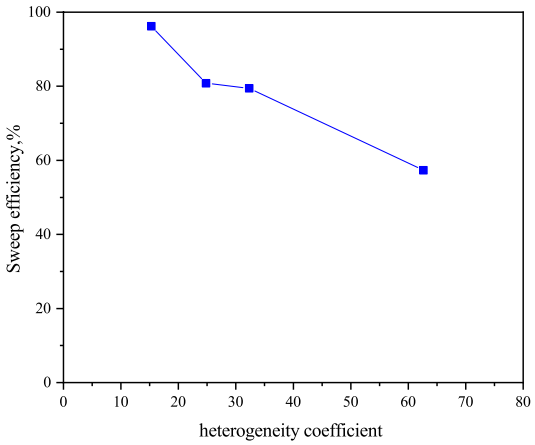

Figure 9. Curve of the heterogeneity coefficient−switch efficiency in the low-viscosity low-velocity group.

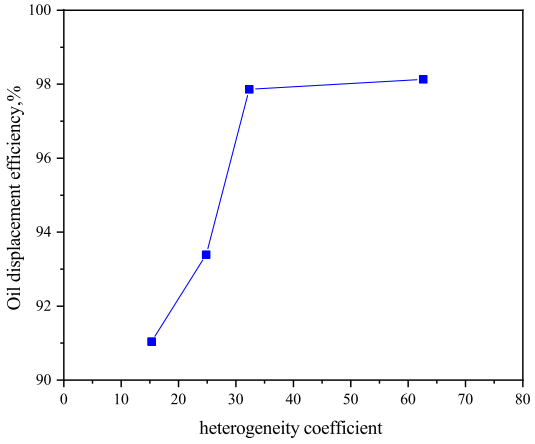

Figure 10. Curve of the heterogeneity coefficient−displacement efficiency in the low-viscosity low-velocity group.

Taking the low-viscosity group as an example, statistics on the recovery degree of sewage flooding under different heterogeneity and capillary number conditions show that, as shown in Figure 11, the results of water flooding recovery degree of different heterogeneity groups all show a pattern of first decreasing and then increasing, with the highest recovery degree of the homogeneous group and the lowest recovery degree of the strong heterogeneity group. With the increase of heterogeneity, the minimum value of recovery degree shifted to the left, that is, the boundary of capillary fingering and viscous fingering shifted to the left, indicating that with the increase of heterogeneity, the trend of viscous fingering in water flooding results became more obvious.

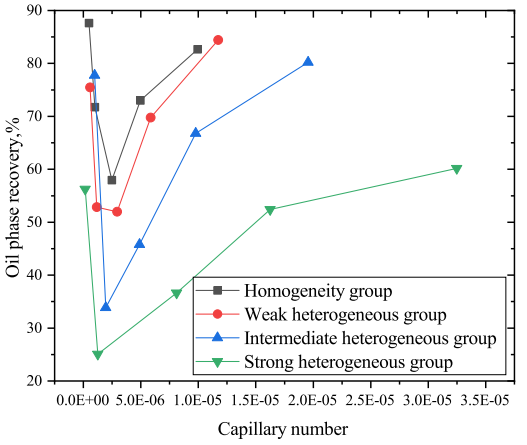

Figure 11. Production degree curves of the low-viscosity group under different heterogeneity and capillary number conditions.

3.4. Classification of the Fluid Intrusion Mechanism.

The distribution of oil and water in a reservoir after water flooding is mainly affected by the fluid intrusion mechanism. Due to the difference of microscopic forces such as capillary force and viscous force, the fluid intrusion mechanism can be divided into two categories: viscous finger and capillary finger. The dominant factors affecting the distributions of oil and water in each fluid intrusion mechanism are different. In the area of viscous fingering, with the increase of capillary number, the effect of viscous force is stronger, and higher displacement power leads to a higher recovery degree. In the area of capillary fingering, under the action of capillary force, the effect of water on pore sweep is better, resulting in a higher recovery degree at low speed. With the increase of the capillary number, the flow of water along large pores has a shielding effect on the pore sweep. The degree of extraction in the capillary inlet area decreases with the increase in capillary number. This phenomenon is also applicable to the high-viscosity group, as shown in Figure 12. For the high-viscosity group with a viscosity of 150 mPa·s, under different heterogeneous conditions, the capillary fingertip is high at the low capillary number and the degree of recovery is high. With the increase of the capillary number, the degree of recovery decreases, while with the increase of the capillary number at medium and high capillary numbers, the degree of recovery increases with the increase of the capillary number, which belongs to the viscous fingertip region.

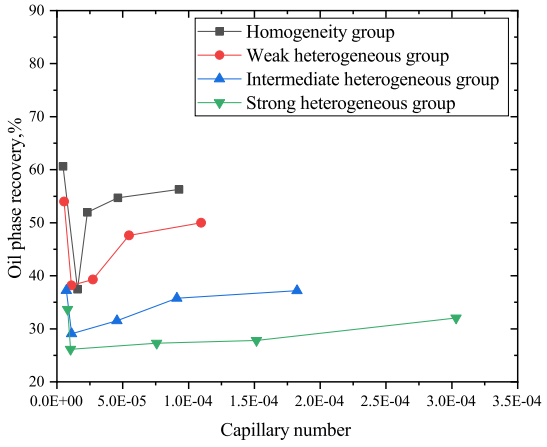

Figure 12. Production degree curves of the high-viscosity group under different heterogeneity and capillary number conditions.

Based on the saturation limit obtained by the experiment, the extraction degree in the capillary fingertip area decreases with the increase of displacement velocity and the extraction degree in the viscous fingertip area increases with the increase of displacement velocity. The capillary number and heterogeneous fluid intrusion mechanism boundary curve at different flow velocities were calculated, as shown in Figures 13 and 14. With the increase of heterogeneity, the viscous fingering trend becomes more obvious. With the increase of viscosity, the fluid

https://doi.org/10.1021/acsomega.3c08205
ACS Omega 2024, 9, 2866−2873

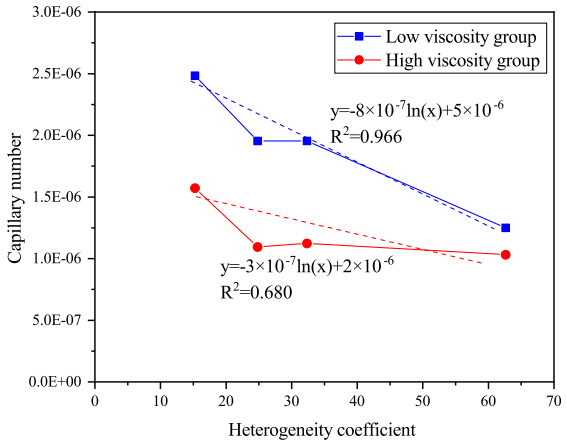

Figure 13. Heterogeneity coefficient−capillary number fluid intrusion mechanism boundary curve.

intrusion mechanism boundary moves down and the viscous fingering trend becomes more obvious.

4. CONCLUSIONS

The fluid intrusion mechanism mainly affects the distribution of oil and water in a reservoir after water flooding. Due to the difference of microscopic forces such as capillary force and viscous force, the fluid intrusion mechanism can be divided into two categories: viscous fingering and capillary fingering. The dominant factors affecting the distribution of oil and water in each fluid intrusion mechanism are different. When capillary fingering occurs, the capillary force of the small hole is stronger, so the sweep is better. With the increase in flow velocity, the large hole has a certain shielding effect on the small hole; therefore, the recovery degree decreases with the increase of flow velocity.

1. As for the influence of flow velocity, when viscous fingering occurs, the viscous force becomes stronger with the increase of flow velocity, and the higher displacement power makes the higher recovery degree. Therefore, the degree of recovery decreases first and then increases with the flow velocity.
2. As for the influence of viscosity, from the numerical point of view, the displacement efficiency and conformance coefficient of the low-viscosity group are higher than those of the high-viscosity group. From the trend, with the increase of the capillary number, the displacement efficiency of both the low-viscosity and high-viscosity groups increases, while the conformance coefficient decreases first and then increases, indicating that capillary fingering and viscous fingering can occur in different viscosity reservoirs.
3. As for the influence of heterogeneity, the conformance coefficient of the water flooding decreases with the increase of heterogeneity, and the viscous pointing trend caused by heterogeneity is stronger, resulting in uneven water injection sweep and higher oil displacement efficiency within the swept area.

Based on the heterogeneous−capillary number curve, it can be seen that the viscous fingering trend becomes more obvious with the increase of heterogeneity and the viscous fingering trend becomes more obvious with the increase of viscosity and the decrease of fingering boundary.

AUTHOR INFORMATION

Corresponding Author

Junjian Li − *College of Petroleum Engineering, China University of Petroleum (Beijing), Changping-qu 102249, China;* orcid.org/0000-0003-0336-8452; Email: junjian@cup.edu.cn

Authors

Jitao Wang − *College of Petroleum Engineering, China University of Petroleum (Beijing), Changping-qu 102249, China;* orcid.org/0009-0001-2178-1171

Yunsong Li − *College of Petroleum Engineering, China University of Petroleum (Beijing), Changping-qu 102249, China*

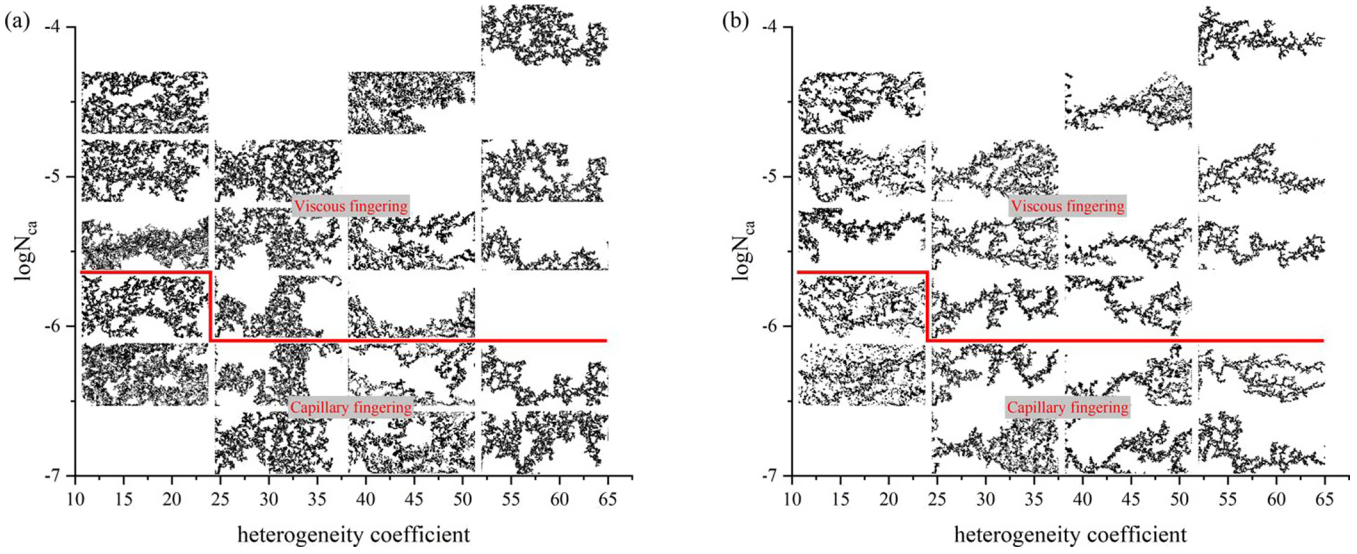

Figure 14. Heterogeneity−capillary number fluid intrusion mechanism classification diagram. (a) Low-viscosity group heterogeneity−capillary number fluid intrusion mechanism classification diagram. (b) High-viscosity group heterogeneity−capillary number fluid intrusion mechanism classification diagram.

https://doi.org/10.1021/acsomega.3c08205
ACS Omega 2024, 9, 2866−2873

Runzi Xu − *College of Petroleum Engineering, China University of Petroleum (Beijing), Changping-qu 102249, China*

Guanghui Xu − *College of Petroleum Engineering, China University of Petroleum (Beijing), Changping-qu 102249, China*

Jinlong Yang − *College of Petroleum Engineering, China University of Petroleum (Beijing), Changping-qu 102249, China*

Complete contact information is available at: https://pubs.acs.org/10.1021/acsomega.3c08205

Author Contributions

J.W.: conceptualization, methodology, writing—original draft, writing—reviewing and editing, conducting experiments; J.L.: supervision, project administration; Y.L.: literature research; R.X.: writing and conducting experiments; G.X.: conducting experiments; J.Y.: recording experimental data.

Notes

The authors declare no competing financial interest.

■ ACKNOWLEDGMENTS

This research was supported by the scientific research project of the Research Institute of Petroleum Exploration and Development and technical support of the China University of Petroleum (Beijing) and Shengli Oil Field Exploration and Development Research Institute.

■ NOMENCLATURE

PV	volume multiple of water flooding in microscopic model, dimensionless
Ca, N_{ca}	capillary number, dimensionless
v,u	velocity of displacing fluid, m/s
σ	interfacial tension over an interface, N/m
μ_i, μ_d	viscosity of displaced and displaced phases, mPa.s
M	viscosity ratio, dimensionless
S_w	wetting saturation, dimensionless
d_z	channel depth of a micromodel, m
k	absolute permeability, m^2
k_{rw}	relative permeability of the wetting phase, dimensionless
θ	contact angle, dimensionless as measured in radians
L_p	length of one pore, m
∇p	magnitude of the macroscopic pressure gradient, Pa/m
W_b	characteristic pore-body diameter, m
W_t	characteristic pore-throat width, m
φ	porosity, dimensionless
ξ	adjustable factor to relate permeability and pore geometry, dimensionless
G	geometric factor for micromodels, dimensionless
f	heterogeneity coefficient, dimensionless

■ REFERENCES

(1) Lenormand, R.; Zarcone.; et al. Mechanisms of the displacement of one fluid by another in a network of capillary ducts. *J. Fluid Mech.* **1983**, *135*, 337.

(2) He, S.; Kahanda, G. L. M. K. S.; Wong, P.-Z.; et al. Roughness of wetting fluid invasion fronts in porous media. *Phys. Rev. Lett.* **1992**, *69* (26), 3731−3734.

(3) Lenormand, R.; Touboul, E.; Zarcone, C.; et al. Numerical models and experiments on immiscible displacements in porous media. *J. Fluid Mech.* **1988**, *189*, 165 DOI: 10.1017/s0022112088000953.

(4) Zhang, C.; Oostrom, M.; Wietsma, T. W.; et al. Influence of Viscous and Capillary Forces on Immiscible Fluid Displacement: Pore-Scale Experimental Study in a Water-Wet Micromodel Demonstrating Viscous and Capillary Fingering. *Acta Ophthalmol.* **2011**, *25* (8), 3493−3505.

(5) Holtzman, R.; Segre, E. Wettability stabilizes fluid invasion into porous media via nonlocal, cooperative pore filling. *Phys. Rev. Lett.* **2015**, *115* (16), No. 164501.

(6) Zhao, B.; Macminn, C. W.; Juanes, R. Wettability control on multiphase flow in patterned microfluidics. *Proc. Natl. Acad. Sci. U.S.A.* **2016**, *113*, 10251.

(7) Hu, R.; Wan, J.; Kim, Y.; et al. Wettability impact on supercritical CO_2 capillary trapping: Pore-scale visualization and quantification. *Water Resour. Res.* **2017**, *53* (8), 6377−6394.

(8) Or, D. Scaling of capillary, gravity and viscous forces affecting flow morphology in unsaturated porous media. *Advances in Water Resources* **2008**, *31* (9), 1129−1136.

(9) Holtzman, R.; Juanes, R.; et al. Crossover from fingering to fracturing in deformable disordered media. *Phys. Rev. E* **2010**, *82* (4), 46305−46305.

(10) Yang, X.; Meng, Y.; Shi, X.; et al. Influence of porosity and permeability heterogeneity on liquid invasion in tight gas reservoirs. *J. Nat. Gas Sci. Eng.* **2016**, *37*, 169.

(11) Dou, Z.; Zhou, Z. F. Numerical study of non-uniqueness of the factors influencing relative permeability in heterogeneous porous media by lattice Boltzmann method. *Int. J. Heat Fluid Flow* **2013**, *42*, 23−32.

(12) Chen, J.-D.; Wilkinson, D.; et al. Pore-Scale Viscous Fingering in Porous Media. *Phys. Rev. Lett.* **1985**, *55* (18), 1892−1895.

(13) King, P. R. The fractal nature of viscous fingering in porous media. *Journal of Physics A General Physics* **1987**, *20* (8), LS29.

(14) Hu, R.; Lan, T.; Wei, G. J. et al. Phase diagram of quasi-static immiscible displacement in disordered porous media. In *AGU Fall Meeting Abstracts*; AGUFM, 2019.

(15) Holtzman, R. Effects of pore-scale disorder on fluid displacement in partially-wettable porous media. *Sci. Rep.* **2016**, *6*, 36221.

(16) Tang, J.; Smit, M.; Vincent-Bonnieu, S.; Rossen, W. R. New Capillary Number Definition for Micromodels: The Impact of Pore Microstructure. *Water Resour. Res.* **2019**, *55*, 1167−1178.